

Research on the post-weld explosive hardening of AA7075-T651 friction stir welded butt joints

Robert KOSTUREK¹ , Rafał LEWCZUK², Janusz TORZEWSKI¹,
Marcin WACHOWSKI¹, Piotr SŁABIK², and Andrzej MARANDA²

¹ Faculty of Mechanical Engineering, Military University of Technology, 2 gen. S. Kaliskiego St., Warsaw, Poland

² Łukasiewicz Research Network – Institute of Industrial Organic Chemistry, 6 Annopol St., Warsaw, Poland

Abstract. In this paper, the post-weld explosive hardening of a 5 mm AA7075-T651 plate welded via FSW was performed. To investigate the possibility of increasing FSW joint mechanical properties, the welded plate was explosively treated with four various explosive materials (ammonal, emulsion explosive, FOX-7, and PBX) in two different hardening systems. As part of the investigation, the observations of the surface and macrostructure of the treated plates were described. The obtained microhardness distribution allowed us to register the increase in hardness of the SZ up to 6%, but no increase in hardness of the LHZ was reported. In most cases, the influence of explosive treatment on the mechanical properties of the welded joint was disadvantageous as ultimate tensile strength and ductility were reduced. The only positive effect which was observed is the increase in the value of yield strength up to 27% corresponding to 77 MPa, achieved by explosive materials with detonation velocity below 3000 m/s.

Key words: aluminum; friction stir welding; explosives; mechanical properties; post-weld treatment.

1. INTRODUCTION

Joining high-strength aluminum alloys requires an appropriate selection of a welding technique to maintain their load-carrying capacities. This issue concerns predominantly elements used in transportation, aircraft, military, and space applications. Friction stir welding (FSW), a solid-state welding process decided for aluminum, can provide high-quality joints of 2XXX and 7XXX alloy series with their joint efficiencies reaching above 75% [1–3]. Recently, many investigations put effort into the post-processing of FSW joints to increase their load-carrying capacities, especially in cyclic loading conditions [4–8]. The applied techniques involve laser peening [4,6], shot peening [7, 8], and cold deformation [5]. It should be mentioned that in the case of conventional welded joints, the post-weld heat treatment (solution treatment and aging) is the most efficient way to almost fully restore the mechanical properties of a precipitation-hardened alloy. Nevertheless, when it comes to FSW joints of 2XXX and 7XXX alloys, the post-weld heat treatment gives undesirable effects (e.g. abnormal grain growth), decreasing fatigue properties of the joints severely [9]. Hence, at this time, the application of a technique based on the post-weld strain hardening of the joint is an appropriate approach. Cabbido *et al.* performed post-weld cold rolling of the AA5754 FSW joint and obtained an increase in the heat-affected zone microhardness by at least 10% [5]. Considering the maintenance of welded workpiece dimensions, the surface-

based techniques: laser and shot peening are more promising, affecting predominantly the fatigue properties of welded joints [7]. The research on laser peening of AA7075-T73 via femtosecond laser was conducted by Kawashima *et al.*, and as the outcome it was stated that the fatigue life of the welded specimen treated with laser beam increases 7 times at the stress amplitude of 200 MPa [4]. A similar research was performed by Toursangsaraki *et al.* on AA2195-T6 alloy, and also, in this case, it was concluded that at the maximum cyclic stress of 250 MPa, the fatigue life of FSW joint treated with laser increases by at least 64% [6]. Bucior *et al.* focused on the shot peening of the 2024-T3 FSW joint and reported that the performed treatment reduces surface roughness, introduces compressive residual stresses, and increases the microhardness of welded zones, which improves fatigue properties [7]. The study done by Ali *et al.* provides results that partially overlap with the previously discussed. The authors investigated the effect of shot peening on the same welded alloy and reported that the fatigue limit increases two times with respect to as-welded samples [8]. The overall conclusion is that the increase in mechanical properties of an FSW joint can be achieved by post-weld treatment in the form of cold plastic deformation or high-pressure shock waves. The high-pressure impulse can be also generated by the detonation of an explosive material. The technique of improving materials properties via the affection of explosives is called explosive hardening and it is predominantly used for strengthening railway crossings and some metallic composites [10–12]. Affecting of a high-pressure shock wave on a treated alloy introduces structural defects impeding the movement of dislocations during plastic deformation [13]. In the FSW of precipitation-hardened aluminum alloys, the crucial

*e-mail: robert.kosturek@wat.edu.pl

Manuscript submitted 2022-12-18, revised 2023-02-24, initially accepted for publication 2023-04-30, published in August 2023.

factors responsible for reducing mechanical properties are the over-aging of the strengthening phase and grain growth which result in the formation of the low-hardness zone (LHZ) [14, 15]. This zone, in most cases, determines the mechanical properties of an FSW joint, so increasing its strength contributes to an entire welded element [16]. For this reason, a potential way to improve joint strength may be the post-weld explosive treatment in which a high-pressure shock wave would increase the hardness of the LHZ. In the current state of the art, there is no research on such post-weld treatment. In this investigation, the aim is to examine the effects of the proposed treatment using different explosives and hardening systems on AA7075-T651 FSW butt joints, in terms of macrostructure, microhardness, and mechanical properties.

2. MATERIALS AND METHODS

The alloy used in this study was AA7075-T651 in the form of 5 mm thick plates. The chemical composition and mechanical properties of the alloy are presented below, in Tables 1 and 2.

Table 1

Chemical composition (weight %) of AA7075-T651 alloy provided by the manufacturer (BIKAR-METALLE GmbH)

Si	Fe	Cu	Mn	Mg	Cr	Zn	Ti	Al
0.07	0.12	1.61	0.025	2.596	0.197	5.69	0.04	Base

Table 2

Mechanical properties of AA7075-T651 alloy

Yield strength, YS	Ultimate tensile strength, UTS	Elongation to break, EL
547.5±1.3 MPa	583.5±1 MPa	14.4±0.6%

The workpieces of AA7075-T651 with dimensions of 80 × 1000 mm have been welded via the FSW technique using the ESAB Legio 4UT machine in the butt joint configuration. The welding parameters were: 400 rpm tool rotation speed and 100 mm/min tool traverse speed (welding velocity). The used tool was the MX Triflute decided for joining 5 mm thick workpieces. The applied welding parameters were the result of the investigation, which is described in detail in the previous work [2]. In the FSW joint three zones can be distinguished: stir zone (SZ), characterized by the presence of ultrafine grains formed in the dynamic recrystallization process, thermo-mechanically affected zone (TMAZ), which was formed in hot plastic deformation, and heat-affected zone (HAZ), which is a part of welded material affected only by the heat of the welding process. Additionally, with respect to the relation between rotation and welding directions, we can distinguish the advancing side (AS), where the linear velocity vector of the rotating tool and the welding direction is the same, and the retreating side (RS), where the linear velocity vector of the rotating tool and the welding direction are opposite to each

other. After the welding process, the pieces with a width about of 200 mm were cut perpendicular to the welding direction in order to perform the explosive hardening. The used system is presented in Fig. 1a and 1b.

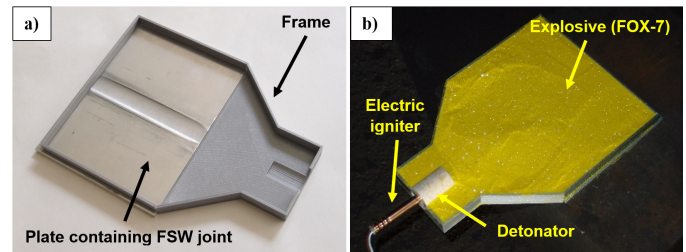


Fig. 1. The explosive hardening system used in this study: FSW joint in the frame (a) and the system filled with explosive and placed electric igniter (b)

The 2 mm thick frame used as an explosive holder (Fig. 1a) was made of polylactic acid via a 3D printing technique. The geometry of the frame was designed to obtain a flat wavefront. In total, four different types of explosives have been used in this investigation: ammonal (10% aluminum powder, 86.5% ammonium nitrate, 3.5% dolomite), emulsion explosive (97% emulsion matrix, 3% glass microspheres), FOX-7 (1,1-diamino-2,2-dinitroethylene), PBX (85% hexogen, 15% polymer matrix). For each of them, the value of detonation velocity has been measured by short circuit sensors and registered by a microsecond counter. The layer of an explosive was 10 mm thick for all materials except PBX which has been used in a 5 mm thick layer. As the electric igniter, the ERGODET M 0.45A has been used (Fig. 1b). A pressed TNT detonator with a mass of 14 g and a diameter of 21 mm has been applied to amplify the initiating impulse. Two different types of explosive hardening systems were used: with an explosive placed directly on the treated element, and another with an additional 1 mm steel sheet as a driven plate. The application of a driven plate allows for obtaining a higher pressure impulse due to high-velocity collision with a treated workpiece [10]. The initial distance between a driven plate and a treated plate was 2 mm. In order to prevent a driven plate from explosively welding with the treated workpiece, the upper surface of the welded plate was covered with a layer of machine oil. The specification of the samples obtained in post-weld explosive treatment is presented in Table 3 below.

After the explosive hardening, the obtained samples were inspected in terms of potential damage and subjected to further analysis. From each plate, three samples for the tensile test and one for the metallographic examination were cut. Metallographic specimens were mounted in resin and subjected to grinding and polishing. The obtained samples were used to establish microhardness distributions on microhardness tester Struers DuraScan 70 applying 0.98 N load in accordance with the ASTM E384 standard. The microhardness was measured at a distance of 0.5 mm from the weld face in order to evaluate the impact of the shock wave on the zones of the welded joint. To reveal the macrostructure of selected samples, Keller's

Table 3

Samples investigated in this study with respect to parameters of used explosive and applied hardening system

Designation (used explosive)	Detonation velocity, m/s	Applied system
As-welded	–	–
Ammonal	2150	Direct
Ammonal + S	2150	Driven steel sheet
Emulsion explosive	4730	Direct
Emulsion explosive + S	4730	Driven steel sheet
FOX-7	5450	Direct
FOX-7 + S	5450	Driven steel sheet
PBX	7300	Direct
PBX + S	7300	Driven steel sheet

reagent was used with a 15-second etching time and chemical composition: 20 mL H₂O, 5 mL 63% HNO₃, 1 mL 40% HF, and one drop of 36% HCl. The macroscopic observations were conducted on the confocal laser scanning microscope OLYMPUS LEXT OLS4100. The tensile tests have been carried out in accordance with the ASTM E8/E8M standard on Instron 8802 MTL supported by WaveMatrix software. The geometry of the tensile samples is presented below in Fig. 2.

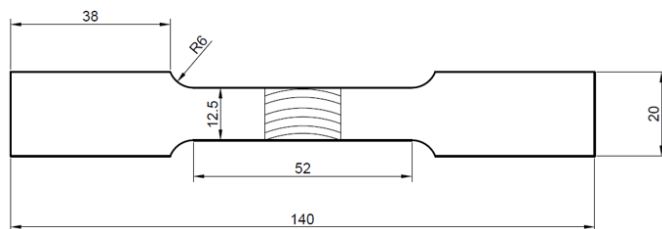


Fig. 2. Scheme of the tensile sample

The fractured surfaces of selected samples were examined on the scanning electron microscope Jeol JSM-6610.

3. RESULTS AND DISCUSSION

The photos of selected, obtained samples are presented in Figs. 3a and 3b.

In general, the performed explosive treatment highly influenced the surface of the welded plate, increasing its roughness and in some cases damaging it. As an example, the welded plate hardened by the emulsion explosive can be considered (Fig. 3a). As can be seen the detonation of the emulsion explosive on the plate created small craters (marked with yellow arrows), which is a result of the Munroe effect in microscale due to the presence of air bubbles on the workpiece surface. The craters did not form in the system with an additional driven steel plate (Emulsion explosive + S sample). For this reason, the application of emulsion explosives in the direct hardening system can be prob-

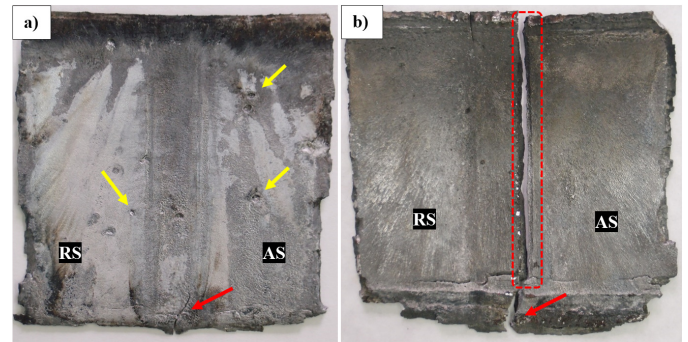


Fig. 3. Explosively hardened samples: Emulsion explosive (a), PBX + S (b)

lematic and requires further research to limit the presence of air bubbles in the emulsion. Also, the edges of treated plates were shorn at 45° angles. Another observation is concerned with the decohesion of the welded joint on the edge of the treated plate (red arrows in Fig. 3a and 3b). The loss of integrity takes place on the SZ/TMAZ interface at the AS. Furthermore, the welded plate hardened by PBX with an additional driven steel sheet has completely lost the integrity of the welded joint in the same zone (red, dashed contour in Fig. 3b). This phenomenon can be explained by the excessively high pressure of the shock wave, which is proportional to the detonation velocity (7300 m/s) and additionally increased by the used driven steel sheet. For this reason, the sample PBX + S was not the subject of further macrostructural and mechanical properties investigation. The last undesirable effect which was obtained during the hardening is explosive welding of the driven sheet to the treated plate in the sample Ammonal + S. Ammonals due to their relatively low values of detonation velocity can be used in explosive welding, for one of the basic requirements is detonation velocity lower than the speed of sound in welded alloys [17, 18]. Nevertheless, the fact that explosive welding took place despite the presence of the machine oil layer, can be a potential problem, and using ammonal as a hardening explosive in this system requires the application of a different covering layer or a driven plate made of plastic.

The macroscopic images of selected samples are presented below in Figs. 4a and 4b.

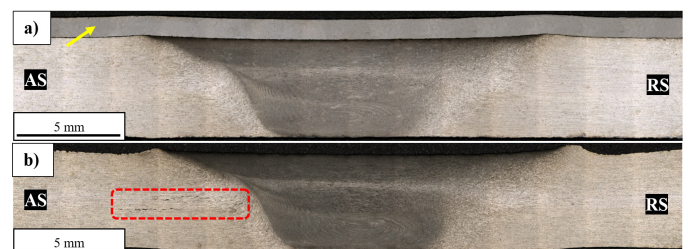


Fig. 4. Macroscopic image of selected samples: Ammonal + S (a), PBX (b)

The first macroscopic image shows the sample, in which a driven sheet has been welded to the treated workpieces (Fig. 4a). As the unintentional result of explosive treatment the

welded clad plate was obtained with the continuous 1 mm layer of steel (yellow arrow in Fig. 4a). For the explosive welding of FSW joints is not the subject of this study, in order to evaluate the impact of hardening on the joint properties the 1 mm cladding was removed before the microhardness measurements and mechanical testing. The plate treated with PBX exhibits the presence of microcracks in the HAZ and TMAZ at AS (red, dashed contour in Fig. 4b), localized about 2.5 mm from the weld face. In the rest of the samples, such defects were not observed. The defects formed in the same area which was the place of decohesion in the PBX + S sample (Fig. 3b), which suggests that the AS is a crucial link in maintaining joint integrity in the condition of explosive loading. The place and the orientation of formed microcracks indicate on affecting of incident shock wave and unloading wave which creates tensile stresses [19]. The failures in PBX and PBX + S samples show that this explosive material has too high detonation parameters to be used in the applied hardening systems. Another important finding is the observed reduction in HAZ thickness as the result of explosive treatment. The changes in thickness are to some point correlated with the detonation velocity of an explosive and the used hardening system. The results of the measurements are presented in Table 4.

Table 4

Measured thicknesses of the HAZ after explosive treatment

Sample	HAZ thickness at AS	HAZ thickness at RS
Ammonal	4.55 mm	4.64 mm
Ammonal + S	4.71 mm	4.71 mm
Emulsion explosive	4.14 mm	4.21 mm
Emulsion explosive + S	4.16 mm	4.34 mm
FOX-7	4.16 mm	4.10 mm
FOX-7 + S	4.21 mm	4.28 mm
PBX	4.39 mm	4.41 mm

The analysis of the performed measurements allows us to draw several conclusions. Firstly, the application of the direct hardening system results in greater thickness reduction than the system with a driven sheet. This is a crucial conclusion from the technological point of view in order to maintain the dimensions of a treated element. Secondly, in most cases, the thickness of AS seems to be more affected than the RS, which can be partially linked to the differences in properties between these two sides [20]. The lowest reduction in thickness was obtained for the explosive with the lowest value of detonation velocity (2150 m/s) – ammonal. The obtained microhardness distributions at a distance of 0.5 mm from the weld face for all analyzed samples are presented in Figs. 5a and 5b.

Although the performed post-weld explosive treatment did not change the shape of the microhardness distribution, maintaining a typical “W”-shape, the hardness of each zone was af-

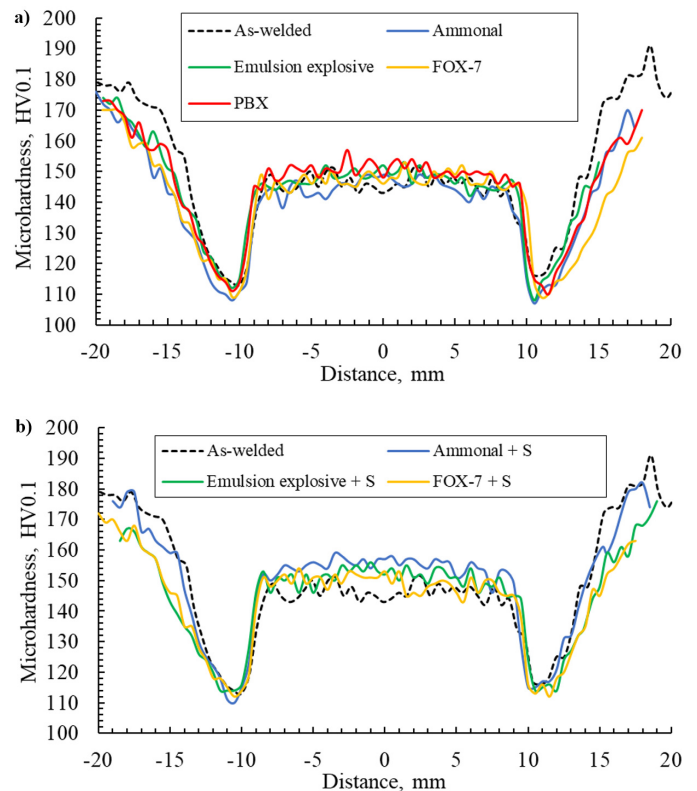


Fig. 5. Microhardness distributions on the treated FSW joints cross-sections: direct hardening system (a) and with a driven steel sheet (b)

ected. Considering the direct hardening system, it can be observed that, generally, applied explosives decrease the value of microhardness in the TMAZ and HAZ (Fig. 5a). An exception is the hardening of the SZ, which has been reported in the case of PBX (Fig. 5a). The average hardness of the SZ in the as-welded sample is 145.1 ± 4.4 HV0.1, for PBX samples it was established as 149.8 ± 2.7 HV0.1 which corresponds to about a 3% increase. The important observation is that opposite to the intended result, the microhardness of the LHZ was slightly reduced by the post-weld explosive treatment from about 115 HV0.1 to 110 HV0.1 depending on the explosive, with the most visible changes at the RS (Fig. 5a). At the same time, the welded plates hardened in the system with a driven sheet are characterized by noticeably higher values of microhardness in the SZ (Fig. 5b). The average microhardness in this zone was established as 154.2 ± 3.2 HV0.1, 150.6 ± 3.2 HV0.1, and 148.8 ± 3.3 HV0.1 for Ammonal + S, Emulsion explosive + S, and FOX-7 + S, respectively. It can be stated that in this type of hardening system, the obtained hardening of the SZ is inversely proportional to the detonation velocity. Also, in this case, the increase in the LHZ microhardness has not been achieved (Fig. 5b), although its reduction is not as high as in the direct hardening system (Fig. 5a). The important conclusion is that the application of the driven plate results in higher hardening at the same time better maintaining the dimensions of the treated workpiece (Table 4). The fact that most of the performed post-weld explosive treatments reduce the microhardness of the FSW joint can be connected with the temperature during the process. As can be

Research on the post-weld explosive hardening of AA7075-T651 friction stir welded butt joints

seen in Fig. 5a also the base material became slightly softer after the treatment, which indicates the unfavorable heat-activated process – over-aging of the strengthening phase. It must be noticed that the source of the heat is not only the affection of hot detonation products but also the compression of treated material during loading by the shock wave. In the case of precipitate-free alloy increase in microhardness is possible, what has been stated by Najwer *et al.* in the research on explosive welding of AA2519 in the annealed condition, obtaining an increase in microhardness from about 75 HV0.1 to 95 HV0.1 [21].

To evaluate the impact of explosive hardening on the mechanical properties of the FSW joint tensile tests have been conducted and the obtained results are presented in Figs. 6a and 6b.

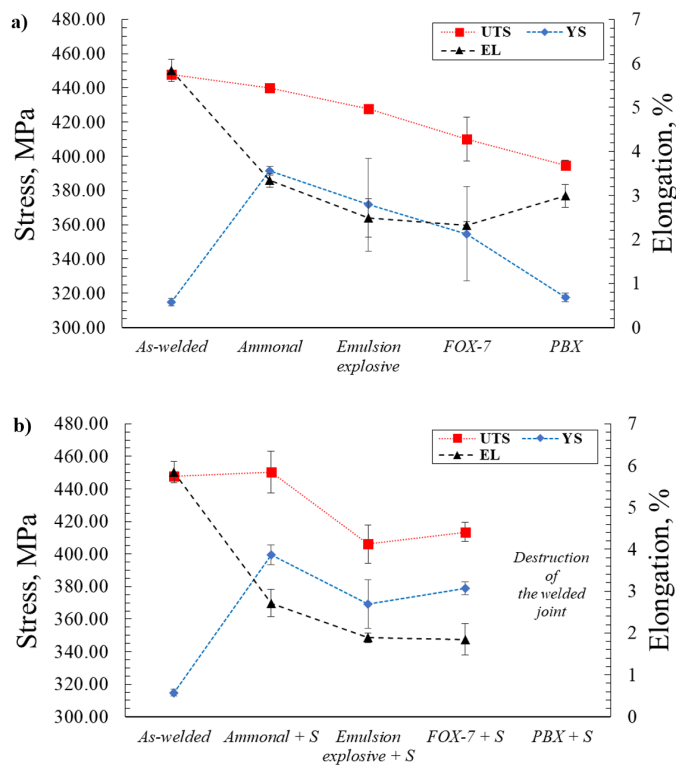


Fig. 6. Established mechanical properties: yield strength (YS), ultimate tensile strength (UTS), and elongation at break (EL) for plates hardened in the direct system (a) and with a driven sheet (b)

The analysis of the obtained results allows us to state that the performed post-weld explosive hardening reduces both UTS and EL values of the FSW joint. In the case of the direct hardening system, the tendency is clear that the higher the detonation velocity the greater decrease in the UTS (Fig. 6a). On the other hand, in the system with a driven plate, the average value of UTS for the Ammonal + S sample suggests that explosive treatment slightly increases this parameter (Fig. 6b). Nevertheless, the rest of the samples hardened via a driven plate exhibit a similar tendency of decreases in UTS and EL. The only, clear positive effect of the proposed treatment is a significant increase in YS in the joints treated with ammonal, emulsion explosive, and FOX-7 (Figs. 6a and 6b). A very similar outcome was obtained by Neu in the investigation on shock hardening of AA7050 us-

ing C-20 explosive (detonation velocity of 5730 m/s), which results in a decrease of UTS by 15 MPa and EL by 6.5% but increases YS by 35 MPa [22]. Referring to Neu's research and the results obtained in this study, it can be concluded that the FSW joints are far more susceptible to explosive treatment than the base material. The relationship between the percentage increase in YS and the detonation of a used explosive is presented below (Fig. 7).

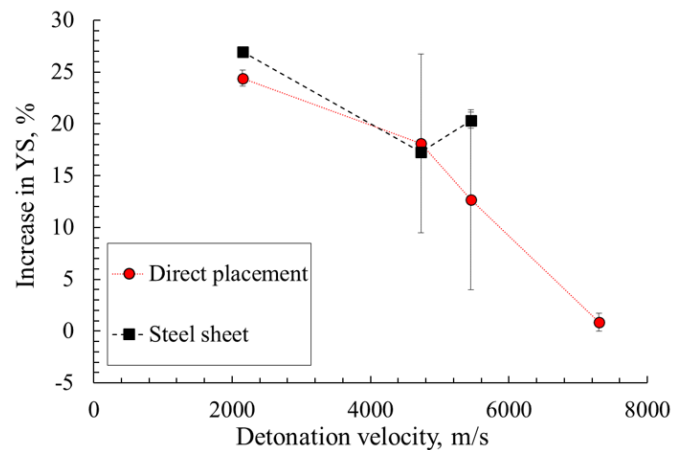


Fig. 7. Relationship between an increase in yield strength and detonation velocity of applied explosive and hardening system

The obtained relationship indicates that in the considered hardening system, the highest increase in YS (above 20%) can be achieved by explosives materials with detonation velocity below 3000 m/s. Based on the mechanical properties of the treated joints, the best outcomes were accomplished by ammonal. It ensures about a 25% increase in YS, maintaining a relatively high value of UTS. The reduction of EL is on a similar level for all used explosives. The problem which must be solved in a technological field is the explosive welding of a driven sheet and the treated workpieces when ammonal is used in such a hardening system. The selected, representative tensile curves for the As-welded sample and the samples treated with ammonal in different hardening systems configurations are presented in Fig. 8.

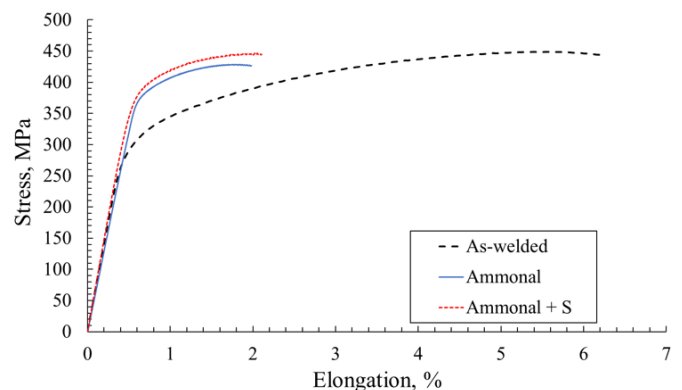


Fig. 8. Representative tensile curves of the FSW joint and the joints treated with ammonal in different hardening systems

The analysis of the presented curves allows us to conclude that the behavior of hardened samples in tensile loading is similar. Despite the significant increase in YS, the lower ductility entails a reduction in the amount of energy that can be absorbed by treated samples. The calculation of areas under the curves indicates at least a 3.3 times reduction in the absorbed energy.

Similar to the As-welded sample, all hardened joints failed in the tensile test in the LHZ at the AS. The selected images of fractured surfaces are presented below in Figs. 9a–9e.

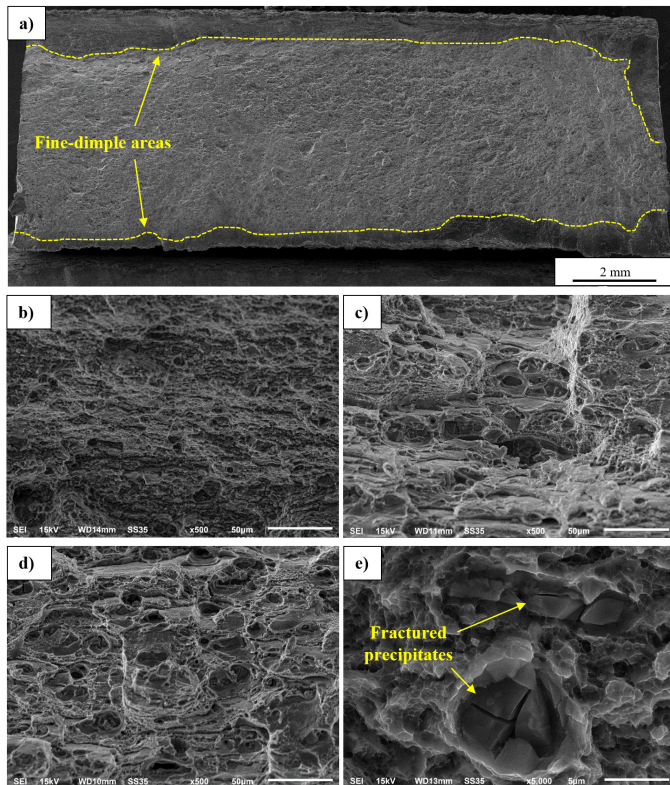


Fig. 9. SEM image of fracture surface: the Ammonal sample – overall view (a), hardened layer (b), dimple structure in the hardened sample (c), dimple structure in the As-welded sample (d), fractured precipitates (e)

The overall view of the Ammonal sample reveals no imperfections which can influence the fracture behavior in this area (Fig. 9a). The fractured surface is homogenous without significant surface irregularities. The SEM observations have allowed us to distinguish two different regions with different dimple sizes: the fine-dimple area, close to the upper and lower surface (Fig. 9b), and the large dimple area in the central part of the fractured sample (Fig. 9c). The fractured character overlaps with the as-welded FSW joint and it is dominated by the transgranular ductile rupture with microvoid coalescence [2]. The formation of fine-dimple structures can be a result of material hardening [23]. In the central part of the fracture surface, the dimples are larger (Fig. 9c) and their size and morphology correspond to the dimple structure in the as-welded joint (Fig. 9d). Additionally, the presence of a large number of fractured precipitates was reported (Fig. 9e).

4. CONCLUSIONS

The performed research allowed us to draw the following conclusions:

1. The post-weld explosive treatment affected the properties of the FSW joint. For all samples, a reduction in HAZ thickness has been reported. The samples treated with PBX (detonation velocity of 7300 m/s) exhibit the presence of microcracks in the HAZ and TMAZ at the AS.
2. The obtained microhardness distribution allowed us to register an increase in hardness of the SZ up to 6% in the case of the samples treated via a driven plate with the hardening inversely proportional to the detonation velocity. No increase in the hardness of the LHZ was reported.
3. In most cases, the influence of explosive treatment on the mechanical properties of the welded joint was disadvantageous as ultimate tensile strength and ductility were reduced. The only positive effect which was observed is the increase in the value of yield strength up to 27% corresponding to 77 MPa, achieved by explosives materials with a detonation velocity below 3000 m/s.
4. The explosive hardening influenced the fractured character of the treated plates, where close to the upper and lower surface the fine-dimple structures were formed by microvoid coalescence.

ACKNOWLEDGEMENTS

This work was financially supported by the National Science Centre (NCN) in Poland, Miniatura 5 no. 2021/05/X/ST8/01480.

REFERENCES

- [1] P. Myśliwiec, R.E. Śliwa, R. Ostrowski, M. Bujny, and M. Zwolak, “Effect of Welding Parameters and Metal Arrangement of the AA2024-T3 on the Quality and Strength of FSW Lap Joints for Joining Elements of Landing Gear Beam,” *Arch. Metall. Mater.*, vol. 65, no. 3, pp. 1205–1216, 2020, doi: [10.24425/amm.2020.133240](https://doi.org/10.24425/amm.2020.133240).
- [2] R. Kosturek, J. Torzewski, M. Wachowski, and L. Śnieżek, “Effect of Welding Parameters on Mechanical Properties and Microstructure of Friction Stir Welded AA7075-T651 Aluminum Alloy Butt Joints,” *Materials*, vol. 15, no. 17, p. 5970, Jan. 2022, doi: [10.3390/ma15175950](https://doi.org/10.3390/ma15175950).
- [3] Z. Wang *et al.*, “Microstructure and Properties of Friction Stir Welded 2219 Aluminum Alloy under Heat Treatment and Electromagnetic Forming Process,” *Metals*, vol. 8, no. 5, p. 305, May 2018, doi: [10.3390/met8050305](https://doi.org/10.3390/met8050305).
- [4] T. Kawashima *et al.*, “Femtosecond Laser Peening of Friction Stir Welded 7075-T73 Aluminum Alloys,” *J. Mater. Process. Technol.*, vol. 262, pp. 111–122, Dec. 2018, doi: [10.1016/j.jmatprotec.2018.06.022](https://doi.org/10.1016/j.jmatprotec.2018.06.022).
- [5] M. Cabibbo, C. Paoletti, M. Ghat, A. Forcellese, and M. Simoncini, “Post-FSW Cold-Rolling Simulation of ECAP Shear Deformation and Its Microstructure Role Combined to Annealing in a FSWed AA5754 Plate Joint,” *Materials*, vol. 12, no. 9, p. 1526, Jan. 2019, doi: [10.3390/ma12091526](https://doi.org/10.3390/ma12091526).

Research on the post-weld explosive hardening of AA7075-T651 friction stir welded butt joints

- [6] M. Toursangsaraki and Y. Hu, "Crystal plasticity evaluation of laser peening effects on improving high-cycle fatigue life of Al-Li friction stir welded joints," *Mater. Des.*, vol. 223, p. 111147, Nov. 2022, doi: [10.1016/j.matdes.2022.111147](https://doi.org/10.1016/j.matdes.2022.111147).
- [7] M. Bucior, R. Kluz, A. Kubit, and K. Ochał, "Analysis of the Possibilities of Improving the Selected Properties Surface Layer of Butt Joints Made Using the FSW Method," *Adv. Sci. Technol. Research Journal*, vol. 14, no. 1, pp. 1–9, 2020, doi: [10.12913/22998624/111662](https://doi.org/10.12913/22998624/111662).
- [8] A. Ali *et al.*, "The effect of controlled shot peening on the fatigue behaviour of 2024-T3 aluminium friction stir welds," *nt. J. Fatigue*, vol. 29, no. 8, pp. 1531–1545, Aug. 2007, doi: [10.1016/j.ijfatigue.2006.10.032](https://doi.org/10.1016/j.ijfatigue.2006.10.032).
- [9] R. Kosturek, L. Śnieżek, M. Wachowski, and J. Torzewski, "The Influence of Post-Weld Heat Treatment on the Microstructure and Fatigue Properties of Sc-Modified AA2519 Friction Stir-Welded Joint," *Materials*, vol. 12, no. 4, p. 583, Feb. 2019, doi: [10.3390/ma12040583](https://doi.org/10.3390/ma12040583).
- [10] J. Nowaczewski, M. Kita, J. Świczak, and J. Rudnicki, "Explosive and thermochemical treatment of multi-layer metallic composites," *High Energy Mater.*, vol. 11, no. 1, pp. 39–44, 2019, doi: [10.22211/matwys/0066E](https://doi.org/10.22211/matwys/0066E).
- [11] F.C. Zhang *et al.*, "Explosion hardening of Hadfield steel crossing," *Mater. Sci. Technol.*, vol. 26, no. 2, pp. 223–229, 2010, doi: [10.1179/174328408X363263](https://doi.org/10.1179/174328408X363263).
- [12] J. Gronostajski and W. Palczewski, "The effects of explosive hardening on the mechanical properties and structure of HSLA steels," *J. Mech. Working Technol.*, vol. 18, no. 3, pp. 293–303, Mar. 1989, doi: [10.1016/0378-3804\(89\)90088-0](https://doi.org/10.1016/0378-3804(89)90088-0).
- [13] N. Djordjevic *et al.*, "Modelling of shock waves in fcc and bcc metals using a combined continuum and dislocation kinetic approach," *Int. J. Plast.*, vol. 105, pp. 211–224, Jun. 2018, doi: [10.1016/j.ijplas.2018.02.014](https://doi.org/10.1016/j.ijplas.2018.02.014).
- [14] K. Mrocza, A. Wójcicka, and A. Pietras, "Characteristics of Dissimilar FSW Welds of Aluminum Alloys 2017A and 7075 on the Basis of Multiple Layer Research," *J. Mater. Eng. Perform.*, vol. 22, no. 9, pp. 2698–2705, Sep. 2013, doi: [10.1007/s11665-013-0570-7](https://doi.org/10.1007/s11665-013-0570-7).
- [15] I. Morozova *et al.*, "Precipitation phenomena in impulse friction stir welded 2024 aluminium alloy," *Mater. Sci. Eng. A*, vol. 852, p. 143617, Sep. 2022, doi: [10.1016/j.msea.2022.143617](https://doi.org/10.1016/j.msea.2022.143617).
- [16] P. Manikandan *et al.*, "Tensile and Fracture Properties of Aluminium Alloy AA2219-T87 Friction Stir Weld Joints for Aerospace Applications," *Metall. Mater. Trans. A*, vol. 52, no. 9, pp. 3759–3776, Sep. 2021, doi: [10.1007/s11661-021-06337-y](https://doi.org/10.1007/s11661-021-06337-y).
- [17] J. Paszula, A. Maranda, B. Kukfisz, and P. Putko, "Investigation of the Explosive Characteristics of Ammonium Nitrate and Aluminium-Magnesium Alloy Powder Mixtures," *Energies*, vol. 15, no. 23, p. 8803, Jan. 2022, doi: [10.3390/en15238803](https://doi.org/10.3390/en15238803).
- [18] Y. Yu, H. Ma, K. Zhao, Z. Shen, and Y. Cheng, "Study on Underwater Explosive Welding of Al-Steel Coaxial Pipes," *Cent. Eur. J. Energ. Mater.*, vol. 14, no. 1, p. 251–265, 2017, doi: [10.22211/cejem/68696](https://doi.org/10.22211/cejem/68696).
- [19] L.-L. Wang, "Unloading waves and unloading failures in structures under impact loading," *Int. J. Impact Eng.*, vol. 30, no. 8, pp. 889–900, Sep. 2004, doi: [10.1016/j.ijimpeng.2003.10.031](https://doi.org/10.1016/j.ijimpeng.2003.10.031).
- [20] R. Kosturek, L. Śnieżek, J. Torzewski, T. Ślęzak, M. Wachowski, and I. Szachogłuchowicz, "Research on the Properties and Low Cycle Fatigue of Sc-Modified AA2519-T62 FSW Joint," *Materials*, vol. 13, no. 22, p. 5226, Jan. 2020, doi: [10.3390/ma13225226](https://doi.org/10.3390/ma13225226).
- [21] M. Najwer and P. Niesłony, "Ocena mikrotwardości oraz własności wytrzymałościowych trimetalu AA2519-AA1050-TI6AL4V po różnych obróbkach cieplnych," *Przegląd Spawalnictwa*, vol. 88, no. 4, p. 16–18, Apr. 2016, doi: [10.26628/ps.v88i4.589](https://doi.org/10.26628/ps.v88i4.589).
- [22] C.E. Neu, "Properties of Shock Hardened 7050 Aluminum Alloy," Naval Air Development Center Warminster Pa Aircraft And Crew Systems Technology Directorate, 1981.
- [23] I. Konovalenko, P. Maruschak, J. Brezinová, and J. Brezina, "Morphological Characteristics of Dimples of Ductile Fracture of VT23M Titanium Alloy and Identification of Dimples on Fractograms of Different Scale," *Materials*, vol. 12, no. 13, p. 2051, Jan. 2019, doi: [10.3390/ma12132051](https://doi.org/10.3390/ma12132051).